Hindawi
Geofluids
Volume 2022, Article ID 4866805, 9 pages
https://doi.org/10.1155/2022/4866805

Research Article

Study on Prediction of Outburst Risk of Excavation Face by Initial Gas Emission

Lu Gao, Xiangtao Kang, Meng Tang, Jinguo Hu, Jiachi Ren, and Cunliu Zhou

Mining College, Guizhou University, Guiyang 550025, China

Correspondence should be addressed to Xiangtao Kang; xiaokangedu@163.com

Received 19 January 2022; Revised 24 February 2022; Accepted 8 March 2022; Published 30 March 2022

Academic Editor: Liang Xin

In order to improve the accuracy of coal and gas outburst risk prediction for an excavation face, an outburst equilibrium equation for the excavation face was established based on the Mohr–Coulomb criterion to predict the coal and gas outburst risk for the excavation face. The numerical model was established using the COMSOL Multiphysics simulation software to explore the relationship between the initial gas emissions from the borehole and the gas pressure. Using a ZTL20/1000-Z mine flameproof prediction device, taking excavation face 9301 in the Anshun Coal Mine in Guizhou Province, China, as the research object, and taking the *detailed regulations for prevention and control of coal and gas outburst* promulgated by the China Coal Mine Safety Supervision Bureau in 2019 as the prediction standard for coal and gas outbursts, an experiment on the outburst risk prediction for the excavation face was conducted. The results show that the gas pressure measured in the borehole is positively correlated with the initial gas emissions, and the initial gas flow can be used as a sensitive index to predict the outburst risk of the excavation face. The initial gas flow increases as the borehole depth increases, and it tends to be stable in the later stage. The initial borehole gas flow can not only reflect the outburst risk but also reveal the possible location of the outburst, which has obvious advantages over other outburst prediction indexes.

1. Introduction

Coal and gas outbursts are a dynamic phenomenon related to the combined action of gas pressure and ground stress on a coal and rock mass containing gas. They are mainly manifested as a large amount of coal and gas rushing to the excavation face in a very short period of time [1]. Numerous studies have shown that the occurrence of a coal and gas outburst requires the destruction of the coal and rock mass under the action of the ground stress to produce a large number of pores and cracks, and then, a large amount of energy is released to the excavation face under the action of the high-pressure gas. Such disasters can result in a large number of casualties and property losses. In short, coal and gas outbursts are a process of energy release [2, 3]. In recent years, with the increase in the coal mining depth in China, the amount of mine gas emission has increased, resulting in occasional coal and gas outburst accidents [4, 5]. Beamish and Crosdale, Liu et al., and Hu and Zhao [6–8] analyzed the mechanism and current situation of coal and gas outburst accidents in mines.

Based on the coal and gas outburst accident mechanism, Lama and Bodziony and Wang et al. [9, 10] proposed a series of effective preventive measures, including a mining protective layer, advanced drilling, and hydraulic punching. However, coal mines defined as outburst mines are not all working areas with outburst risks. On the contrary, coal and gas outbursts often occur only in local areas in the mine [11–13]. Therefore, it is of great importance to accurately predict whether their excavation face is at risk of a coal and gas outburst. Gas emissions have long been considered to be a complex engineering system. It is difficult to effectively, comprehensively, and accurately predict the risk of coal seam gas outbursts using a single index, and then, the reliability is not guaranteed, which has certain limitations. Dynamic prediction can comprehensively reflect the risk of coal seam outbursts near a coal body, and

it has a higher accuracy for the prediction of gas emissions from a coal mining face.

Cheng et al. [14] established the relationship between the gas desorption index for drill cutting Dh2 and the gas pressure in the coal seams. Gui et al. [15–17] discussed the influencing factors, including the quantity of drilling cuttings and the gas desorption index of the drilling cuttings, in predicting the risk of coal and gas outbursts. Tan et al. [18] analyzed the problem of how to reflect the stress of a coal body using drilling cuttings according to the Mohr–Coulomb criterion.

Cao and Wang [19] proposed the incremental change index for drilling cuttings under a stress gradient by considering factors such as the expansion factor and obtained the relationship between the drilling cuttings and coal stress. At present, the indicators used to identify whether an excavation face has a prominent risk generally include the drilling cutting bit index, the temperature index, and the composite index [20–22]. However, the above prediction indexes are all static prediction indexes, and the dynamic prediction indexes for predicting the outburst risk for an excavation face have rarely been studied [23].

Based on this, in this study, a numerical model was developed based on theoretical analysis, and the conditions of coal and gas outbursts from an excavation face and the relationship between the borehole gas emissions and gas pressure were investigated. Using a ZTL20/1000-Z type mining flameproof outburst prediction device and taking excavation face 9303 in the Anshun Coal Mine in Guizhou Province as the experimental object, field research on outburst prediction was carried out in order to develop a new method for predicting the risk of coal and gas outburst from an excavation face.

2. Engineering Background and Experimental Equipment

2.1. Engineering Background. Excavation face 9303 is located in coal seam #9 in a three-panel area, which is the main coal seam in the Anshun Coal Mine in Guizhou Province, China. The average thickness of the coal seam is 1.6 m, and the coal seam is relatively stable. There is no false roof in the coal seam roof. The immediate roof is composed of silty mudstone, with a thickness of 5.27 m. The old roof is composed of limestone, with a thickness of 4.79 m. The immediate roof is composed of argillaceous siltstone, with a thickness of 3.78 m. The old floor is composed of silty mudstone, with a thickness of 8.12 m. The coal seam's geographical location and a mining histogram are shown in Figure 1.

In 2018, the basic parameters of the gas in coal seam #9 in the Anshun Coal Mine in Guizhou Province were measured by the Safety Production Testing and Inspection Center of the China University of Mining and Technology. The maximum gas content of the coal seam was 9.2 m^3/t, the maximum gas pressure was 0.77 MPa, the permeability coefficient was 0.0932-0.1458 m/MPa·d, the initial velocity of the gas released was 25–32 m/s, and the firmness coefficient was 0.81–0.85.

2.2. Experimental Equipment. A ZTL20/1000-Z type mining flameproof flow method coal seam outburst prediction device was used in the experiments. The device is mainly composed of an air drill, drill bit, twist drill pipe, capsule, manual pressure pump, filtering device, velocity sensor, coal bunker, displacement sensor, and intrinsically safe acquisition host. A schematic diagram of the device is shown in Figure 2.

2.3. Experimental Procedure. The sealing effect of the device is needed to meet the industrial demand under laboratory conditions. The experiment procedures were as follows.

(1) A 42 mm diameter borehole was drilled in the middle of the excavation face

(2) A manual pressure experiment pump was used to inject water into the capsule to seal the hole, and the pressure applied was 3.5 MPa

(3) The sensor was placed in a reserved position, and then, the host was opened, and the data acquisition process was run

(4) The drill bits were placed in the predetermined position in front of the excavation face

(5) The data processing program was run, and the results were output

2.4. Data Processing Method. According to the experimental procedure, the computer program automatically converted the current value of the sensor into the corresponding data curve. The principle of the data processing program is shown in Equations (1) and (2).

$$S_i = \int_{x_1}^{x_2} q_i dx X = \frac{\sum_{i=1}^{n} (S_i \cdot x_i)}{\sum_{i=1}^{n} S_i}, \tag{1}$$

$$M = S \cdot L = S(K_2 - X). \tag{2}$$

S_i is the area for a point in a bore hole (L·m/min). x_1 and x_2 are the distances from both ends of the flow segment at point i to the excavation face (m). q_i is the instantaneous gas flow corresponding to i point (L/min). R is the center of the face of the flow area of the microsegment corresponding to point i. X is the length of the excavation face (m). M is the maximum flow peak area (L·m^2/min). S is the area of the maximum displacement flow curve per unit length (L·m/min). L is the center of gravity distance of the maximum displacement flow curve per unit length and is used to predict the distance to the bottom of the borehole (m). K_2 is the total length of the borehole (m).

It can be seen from Equation (2) that the maximum flow peak area is proportional to the flow area per unit borehole length, and it is inversely proportional to the distance from the center of the surface to the excavation face of the flow area per unit borehole length, that is, the larger the maximum flow peak area of the excavation face is, the more likely it is that a coal and gas outburst will occur.

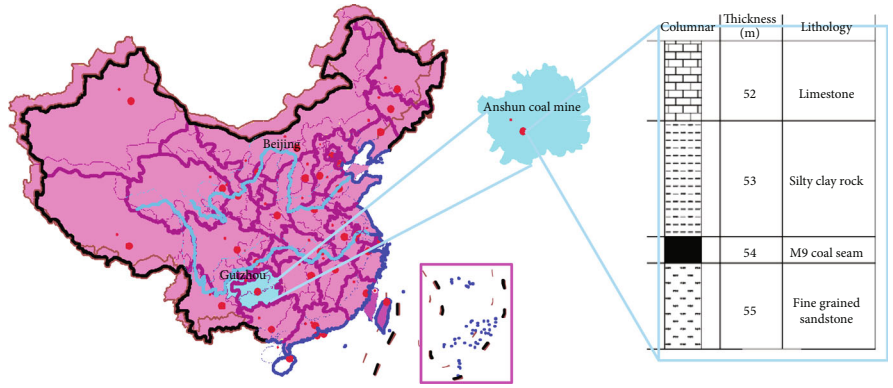

Figure 1: Geographical location of the experimental coal seam and the geographic conditions of the coal seam.

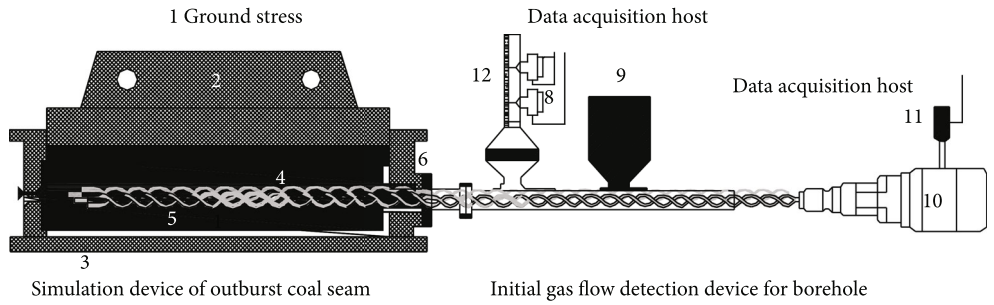

Figure 2: Experimental device. 1—press machine; 2—pressure pole; 3—cylindrical block; 4—drill pipe; 5—coal seam; 6—stopper; 7—large flow sensor; 8—small flow sensor; 9—coal bunker; 10—electric coal drill; 11—displacement sensor; 12—flow tube.

2.5. Initial Gas Emission Law

2.5.1. Construction of Numerical Simulation. In the excavation of a coal roadway, outbursts often occur when the soft layer is exposed near hard coal. This is because the existence of a soft layer not only reduces the tensile strength of the coal, but the ground stress also tends to compress the soft layer, resulting in a decrease in the coal's permeability [24]. The smaller coal permeability causes a large amount of gas to accumulate and form a high-pressure gas source. When the soft layer is suddenly exposed, due to the existence of a pressure difference, a large amount of gas is released into the excavation space in a short period of time, thus creating the conditions of a coal and gas outburst [25–28].

The drilling of a coal mine excavation face is very similar to that of coal mine roadway excavation. When the borehole advances to a soft layer containing a high-pressure gas source, the gas emissions in the borehole increase sharply due to the release of a large amount of gas. The gas emission is shown in Figure 3.

In order to study the relationship between the gas emission from the borehole and the gas pressure, a mathematical model of the source of the borehole gas was established. In this model, the initial drilling gas flow of the gas emission is mainly divided into three parts: the gas flow emitted near the bit, the gas flow emitted from the borehole wall during the drilling process, and the gas flow emitted from the coal dust during the drilling process. Gas emission during drilling is a very complex process [29–33]. Therefore, the following assumptions were made in the model to take into account the main factors [34–40].

(1) The gas in the coal seams is sealed in the coal seams

(2) There are no cracks in the coal seams

(3) The gas in the coal is an ideal gas and obeys Darcy' s law

(4) The coal seam is homogeneous, and the temperature of the coal mass remains constant

(5) The gas permeability of the coal seam does not change with gas pressure

(6) The gas flow around the borehole is spherical unstable flow

When the drill bit begins to drill into the coal seam, the gas flow channel forms near the drill bit first, and the gas near the drill bit obeys spherical seepage under a high gas pressure gradient. The spherical seepage of the gas in the borehole is as follows:

$$\frac{\partial p_0}{\partial t} = a_1 \left[\frac{\partial^2 p}{\partial r^2} + \frac{2\partial p}{r\partial r} \right]. \tag{3}$$

Initial conditions are as follows: $t = 0$时, and $p = p_0 = p_0^2$.

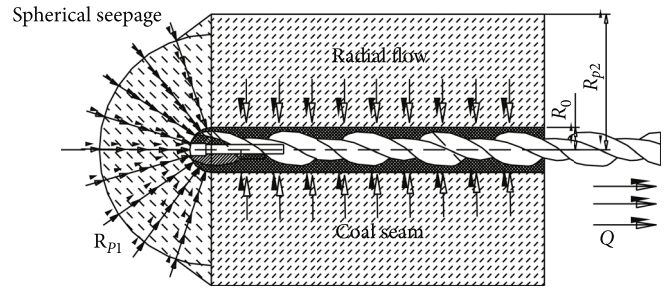

Figure 3: Schematic diagram of gas emission from a borehole.

Boundary conditions are as follows:

$$\begin{cases} 0 \le t < \infty, r = R_1, P = P_1 = p_1^2, \\ 0 \le t < \infty, r \longrightarrow \infty, P = P_0 = p_0^2, \dfrac{\partial P}{\partial r} = 0. \end{cases} \tag{4}$$

According to the Laplace transform, Equation (5) can be obtained as follows:

$$rT(r,S) - \frac{rP_0}{s} = (Ac + Bs)\frac{S}{a_1} rh. \tag{5}$$

The initial conditions and boundary conditions are substituted into Equation (5) to obtain Equation (6):

$$E_0 = \frac{P - P_1}{P_0 - P_1} = 1 - \frac{R_1}{r} \operatorname{erf}\left(\frac{r - R_1}{2\sqrt{a_1 t}}\right). \tag{6}$$

The gas emission equation for the coal wall based on Darcy's Law is as follows:

$$q = -\lambda \left.\frac{\partial P}{\partial r}\right|_{r=R_1}. \tag{7}$$

Substituting Equation (6) into Equation (7) gives

$$q = (p_0 - p_1)\left[\frac{r}{R_1} + \sqrt{\frac{\lambda a}{4\pi p_0^{1.5} t}}\right]. \tag{8}$$

Because the bore hole radius is small relative to the thickness of the coal seam, the borehole can be regarded as an infinitely small hole, and the gas flow around the drilling hole is radial unstable flow. The radial seepage of the gas in the borehole can be described as follows:

$$\frac{\partial P}{\partial t} = a_1\left[\frac{\partial^2 P}{\partial r^2} + \frac{1}{r}\frac{\partial P}{\partial r}\right]. \tag{9}$$

Initial conditions are as follows: $t = 0$, and $P = P_0 = {P_0}^2$.

Boundary conditions are as follows:

$$\begin{cases} 0 < t < \infty, r = R_1, P = P_1 = p_1^2, \\ 0 < t < \infty, r \longrightarrow \infty, P = P_0 = p_0^2, \dfrac{\partial P}{\partial r} = 0. \end{cases} \tag{10}$$

According to the Laplace transform,

$$rT''(r,S) + T'(r,S) + \frac{s}{a_1} r\left[T'(r,S) - \frac{p_0}{S}\right] = 0. \tag{11}$$

The initial conditions and boundary conditions can be substituted into Equation (11) to obtain Equation (12):

$$\frac{P_0}{s} - T(r,S) = \frac{P_0 - P_1}{s}\frac{r}{r_t}. \tag{12}$$

By applying a dimensionless transform to Equation (9), we obtain

$$q = \frac{\lambda Y(P_0 - P_1)}{R_1}. \tag{13}$$

During the drilling of the borehole, the coal body gradually forms coal cuttings after continuous destruction, and the gas flow from the coal cuttings gradually increases. Assuming that the coal cuttings are spherical, isotropic, and homogeneous, the diameter of the coal cuttings remains unchanged during the drilling and conforms to the law of mass conservation during the drilling. Based on the above assumptions, the gas flow from the coal cuttings in the borehole is as follows:

$$\frac{\partial P}{\partial t} = a_1\left(\frac{\partial^2 P}{\partial r^2} + \frac{2}{r}\frac{\partial p}{\partial r}\right). \tag{14}$$

Initial conditions are as follows: $t = 0$, and $P = P_0 = {P_0}^2$. Boundary conditions as follows:

$$\begin{cases} r = R_1 (t > 0), P = P_1 = p_1^2, \\ r = 0 (t > 0), \dfrac{\partial p}{\partial r} = 0. \end{cases} \tag{15}$$

The initial conditions and boundary conditions can be

Table 1: Model parameters.

Borehole diameter (mm)	Length (m)	Elasticity modulus (MPa)	Cohesion (MPa)	Internal friction angle (°)	Poisson ratio	Coal body's tensile strength (MPa)	Coal density ($kg \cdot m^{-3}$)	Dynamic viscosity of gas (Pa·s)	Density of gas ($kg \cdot m^{-3}$)	Temperature (K)
40	1.5	677	2.2	35	0.3	2.2	1300	1.85e-5	0.726	305

substituted into Equation (14), and dimensionless changes are made to obtain Equation (16):

$$E_0 = 1 - \frac{R_1}{r}\left[\text{erf}\left(\frac{1 - r/R_1}{2\sqrt{F_0}}\right) - \text{erf}\left(\frac{1 + r/R_1}{2\sqrt{F_0}}\right)\right]. \quad (16)$$

According to Darcy's law, the gas flow from the drilling cuttings in the borehole can be obtained by changing Equation (16) into Equation (17):

$$q = \frac{\lambda}{2R_1\sqrt{F_0}}(P_0 - P_1)[\exp(-F_0) + 1]. \quad (17)$$

F_0 is the dimensionless time. Y is a dimensionless number. q is the initial gas emission per unit area ($m^3/(m^2 \cdot d)$). λ is the permeability coefficient of the coal seam (MPa). p is the gas pressure of the coal seam (MPa). p_0 is the initial gas pressure of the coal seam (MPa). p_1 is the gas pressure of the borehole (MPa). t is the time (s). R_1 is the radius of the borehole (m). P is the square of p (MPa^2). P_0 is the square of p_0 (MPa^2). P_0 is the square of p_1 (MPa^2).

2.6. Research Based on Numerical Simulation. The boundary conditions of the experimental model indicate that the lower boundary is simplified as a fixed boundary; and the left, right, and rear sides are normal displacement constraint boundaries. The front part is free space, and the upper part is loaded with a stress boundary, namely, the self-weight of the overlying strata. The permeability of the coal seam is a function of the effective stress [41–45]. The specific parameters of the model and the simulation results are presented in Table 1 and Figure 4.

In order to study the gas emission characteristics during the drilling of the excavation face under different pressures, simulations were conducted under the following conditions: a coal seam burial depth of 800 m, a drilling length of 1 m, a drilling time of 4 min, a coal water content of 5.63%, and gas pressures of 0.5 MPa, 1.0 MPa, 1.5 MPa, 2.0 MPa, 2.5 MPa, and 3.0 MPa. The relationship between the gas emission from the borehole and the gas pressure is shown in Figure 5.

It can be seen from Figure 5 that under the different gas pressures, the initial gas emission increased rapidly as the drilling progressed. During the entire drilling process, the gas emission was positively correlated with the gas pressure. Therefore, the gas emission from the borehole can represent the gas pressure, and it can be used as a sensitivity index to determine whether the excavation face has a risk of outburst. Gao et al. [46–49] reported that the total gas emission from a borehole can be used to characterize the initial gas flow from the borehole, and the initial gas emission from the borehole is dynamically measurable as the depth of the borehole drilled in the coal. Therefore, in order to determine if the index of the initial borehole gas flow can be used to predict whether the coal body in front of the excavation face has a risk of outburst, a field experiment was carried out.

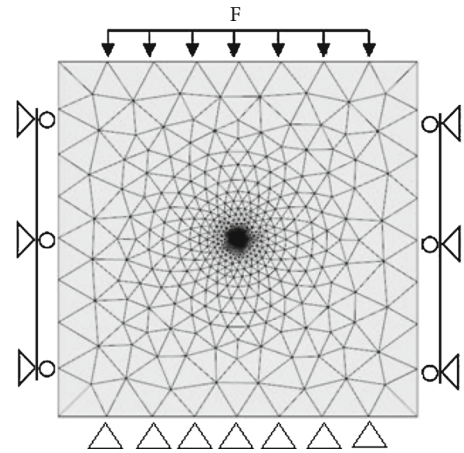

Figure 4: Three-dimensional numerical model.

3. Analysis and Discussion of Experimental Results

In order to ensure sufficient safety distance, the drilling length was 8 m. A total of 12 groups of experimental data were collected. Due to the similarity of the data, one group of experimental data was randomly selected for analysis. The results of the 11 groups are presented in Table 2.

The relationship between the borehole displacement and gas flow is shown in Figure 6. As can be seen from Figure 6, in the early stage of the drilling of the excavation face, the gas flow from the borehole was small and the emission was stable. As the borehole depth increased, the initial gas flow from the borehole began to increase significantly, and then, it became stable. When the drill bit drilled to 3–6 m, the initial gas flow gradually increased, and it reached the maximum value of 13.12 $L \cdot m^2$ at 5–6 m, indicating that there was a large amount of gas adsorbed in the coal seam. When the coal seam was destroyed by the drilling, a large amount of gas was released from the coal seam into the borehole. The maximum flow peak area was 91.63 $L \cdot m^2$/min. Coal samples were collected between 5 m and 6 m. In addition, the maximum drilling cutting bit index and the maximum initial velocity index of the borehole gas emission were used to test and

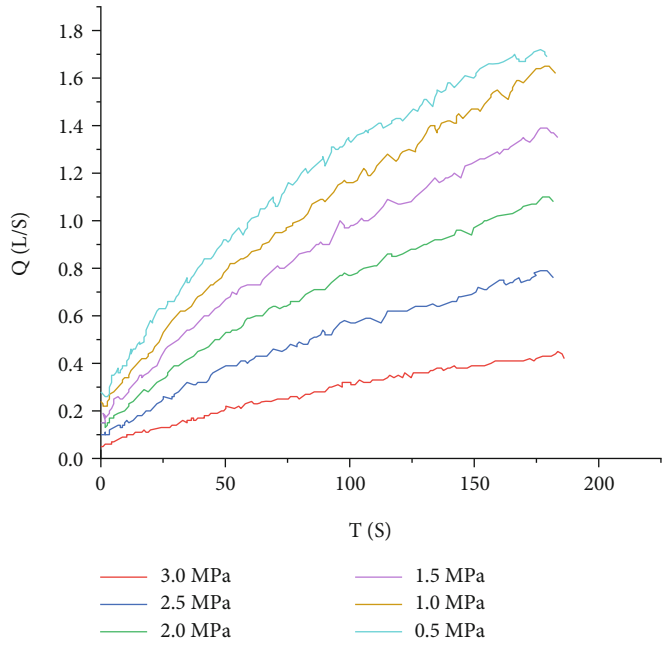

Figure 5: Relationship between the gas emission and gas pressure in the borehole.

Table 2: Experimental results.

Experimental dataset	Maximum drilling cutting bit index ($kg \cdot m^{-1}$)	Maximum gas emission initial velocity index ($L \cdot min^{-1}$)	Maximum flow peak area index ($L \cdot m^2 \cdot min^{-1}$)	With and without coal and gas outburst	Drill became stuck
1	4.5	3.2	142.94	Without	Yes
2	2.6	2.2	13.96	Without	No
3	2.5	2.0	27.87	Without	No
4	2.3	1.7	22.65	Without	No
5	2.4	2.1	94.84	Without	No
6	1.8	3.1	16.68	Without	No
7	2.2	1.7	30.46	Without	No
8	1.8	1.9	9.71	Without	No
9	2.0	2.1	12.15	Without	No
10	1.5	1.2	3.85	Without	No
11	2.2	1.8	20.17	Without	No

judge whether there was a risk of outburst. The measured values of these indexes were 2.34 kg/m and 2.21 L/min, respectively. Both were below the critical values of 6.0 kg/m and 4.0 L/min for these indexes, respectively, according to the *coal and gas outburst prevention rules*. Finally, the prediction section was excavated, and the results show that there was no outstanding phenomenon, that is, when the maximum flow peak area was 91.63 $L \cdot m^2$/min, there was no outburst risk for the excavated coal face.

The experimental results of the other groups are presented in Table 2. The trends of the test results of the maximum flow peak area index, the maximum drilling cutting bit index, and the maximum gas emission initial velocity index of the borehole are basically the same, and the range of the maximum flow peak area for the index is relatively wide. Although there was no outburst from the coal seam during the tunneling process, when the maximum flow peak area was 142.94 $L \cdot m^2$/min, the maximum drilling cutting was 4.5 kg/m and the maximum initial gas emission velocity was 3.2 L/min, which was very close to the critical values of 6.0 kg/m and 4.0 L/min, respectively, as stated in the *Coal and Gas Outburst Prevention and Control Regulations*. In addition, the drill was stuck. Therefore, the maximum flow peak area of 142.94 $L \cdot m^2$/min can be used as a critical value to judge whether there is a risk of outburst in the tunneling of the coal roadway.

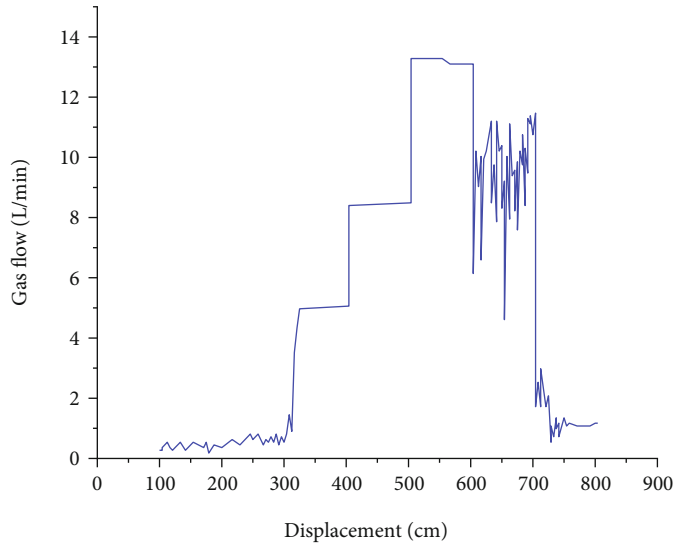

Figure 6: Plot of bore displacement versus gas flow.

4. Conclusions

(1) There is a significant linear relationship between the gas pressure in the borehole and the initial gas flow from the excavation face, so the initial gas flow from the borehole can be used as a sensitive index to predict the outburst risk of the excavation face

(2) The initial gas flow increases as the drilling length increases, and it tends to be stable in the later stage. When the coal seam is exposed and destroyed instantaneously, a large amount of gas will be released. Therefore, the peak area of the gas flow can not only reflect the risk of a coal and gas outburst but also be used to effectively predict the areas where coal and gas outbursts may occur, which has obvious advantages compared with other outburst prediction indexes

(3) The trends of the maximum flow peak area index, the maximum drilling cutting bit index, and the maximum gas emission initial velocity index obtained from the experiments are basically the same, and the range of the maximum flow peak area index is wide. A maximum flow peak area of 142.94 $L \cdot m^2/min$ can be used as the critical threshold for outburst prediction for an excavation face in the Anshun Coal Mine, Guizhou Province, China

Data Availability

The data used to support the findings of this study are included within the article.

Conflicts of Interest

The authors declare that they have no conflicts of interest.

References

[1] J. Tang, C. L. Jiang, Y. J. Chen, X. Li, G. Wang, and D. Yang, "Line prediction technology for forecasting coal and gas outbursts during coal roadway tunneling," *Journal of Natural Gas Science Engineering*, vol. 34, pp. 412–418, 2016.

[2] C. L. Jiang and Y. Q. Xu, "Rules of energy dissipation in coal and gas outburst," *Journal of China Coal Society*, vol. 2, pp. 173–178, 1996.

[3] C. L. Jiang, L. H. Xu, X. W. Li et al., "Identification model and indicator of outburst-prone coal seam," *Rock Mechanics and Rock Engineering*, vol. 48, no. 1, pp. 409–415, 2015.

[4] X. He and L. Song, "Status and future tasks of coal mining safety in China," *Safety Science*, vol. 50, no. 4, pp. 894–898, 2012.

[5] Y. F. Zhu, D. M. Wang, Z. L. Shao et al., "A statistical analysis of coalmine fires and explosions in China," *Process Safety and Environmental Protection*, vol. 121, pp. 357–366, 2019.

[6] B. B. Beamish and P. J. Crosdale, "Instantaneous outbursts in underground coal mines: an overview and association with coal type," *International Journal of Coal Geology*, vol. 35, no. 1-4, pp. 27–55, 1998.

[7] Y. J. Liu, L. Yuan, J. H. Xue, Z. C. Tian, C. R. Duan, and B. L. Chen, "Research status and development trend of mechanism and simulation test of coal and gas outburst," *Industry and Mine Automation*, vol. 44, no. 2, pp. 43–50, 2018.

[8] Q. T. Hu and X. S. Zhao, "Present situation of coal and gas outburst accidents in China's coal mines and countermeasures and suggestions for their prevention," *Mining Safety and Environmental Protection*, vol. 39, no. 5, 2012.

[9] R. D. Lama and J. Bodziony, "Management of outburst in underground coal mines," *International Journal of Coal Geology*, vol. 35, no. 1-4, pp. 83–115, 1998.

[10] F. Wang, P. Zhang, B. Cui, Z. Sun, and K. Zhang, "Research progress of disaster factors and a prevention alarm index of coal and gas outbursts," *Arabian Journal Geosciences*, vol. 14, p. 2042, 2021.

[11] S. Khristianovich, "Distribution of gas pressure close to an advancing coal face," *Irv ANUSSR Otd Tekhn Nauk*, vol. 12, pp. 1673–1678, 1953.

[12] T. Xu, C. Tang, T. Yang, W. C. Zhu, and J. Liu, "Numerical investigation of coal and gas outbursts in underground collieries," *International Journal of Rock Mechanics and Mining Sciences*, vol. 43, no. 6, pp. 905–919, 2006.

[13] Q. T. Hu, G. C. Wen, and S. M. Xu, "Sensitive index and critical value of outburst prediction in excavation face," *Coal Engineer Supplementary*, vol. S1, pp. 8–10, 1998.

[14] L. B. Cheng, L. Wang, Y. P. Cheng, K. Jin, W. Zhao, and L. S. Sun, "Gas desorption index of drill cuttings affected by magmatic sills for predicting outbursts in coal seams," *Arabian Journal of Geosciences*, vol. 61, no. 9, 2015.

[15] X. Y. Gui, Y. L. Xu, X. Y. Meng, and Z. M. Yu, "Application of the value of drilling cuttings weight and desorption index for drill cuttings to preventing coal and gas outburst," *Chinese Journal of Engineering*, vol. 31, no. 3, pp. 285–289, 2009.

[16] G. Z. Yin, X. Q. Li, H. B. Zhao, X. S. Li, and G. S. Li, "In-situ experimental study on the relation of drilling cuttings weight to ground pressure and gas pressure," *Chinese Journal of Engineering*, vol. 32, no. 1, pp. 1–7, 2010.

[17] Z. Sun, L. Li, F. Wang, and G. Zhou, "Desorption characterization of soft and hard coal and its influence on outburst prediction index," *Energy Sources Part A Recovery Utilization and Environmental Effects*, vol. 2, pp. 1–15, 2019.

[18] J. Tan, T. Yan, Z. Wang, and Y. Zhang, "Identification for abutment stress by drilling cuttings," *Applied Sciences*, vol. 11, no. 20, 2021.

[19] Y. L. Cao and M. Wang, "Sensitivity and its critical value of gas desorption index △h2 in coal drilling cutting at Panyi coal mine. Journal of Liaoning Technical University," *Natural Science Edition*, vol. 30, no. 5, pp. 685–688, 2011.

[20] X. Sun and D. Sun, "Trial study of determining critical values of outburst prediction indicators value K_1 and f," *Mining Safety & Environmental Protection*, vol. 27, no. 4, pp. 23–26, 2000.

[21] S. Tian, C. Jiang, L. Xu et al., "A study of the principles and methods of quick validation of the outburst-prevention effect in the process of coal uncovering," *Journal of Natural Gas Science and Engineering*, vol. 30, pp. 276–283, 2016.

[22] D. Li, Y. Cheng, L. Wang, H. Wang, L. Wang, and H. Zhou, "Prediction method for risks of coal and gas outbursts based on spatial chaos theory using gas desorption index of drill cuttings," *Mining Science and Technology*, vol. 21, no. 3, pp. 439–443, 2011.

[23] C. J. Wang, S. Q. Yang, X. W. Li, D. Yang, and C. Jiang, "The correlation between dynamic phenomena of boreholes for outburst prediction and outburst risks during coal roadways driving," *Fuel*, vol. 231, pp. 307–316, 2018.

[24] Y. G. Wang, J. P. Wei, and H. T. Sun, "Mechanism analysis of coal or rock dynamic disaster and its prevention and control," *Mining Safety & Environmental Protection*, vol. 37, no. 2, pp. 17–19, 2010.

[25] D. D. Yang, Y. J. Chen, J. Tang et al., "Experimental research into the relationship between initial gas release and coal-gas outbursts," *Journal Natural Gas Science Engineering*, vol. 50, pp. 157–165, 2018.

[26] X. W. Li, C. L. Jiang, J. Tang, Y. Chen, D. Yang, and Z. Chen, "A Fisher's criterion-based linear discriminant analysis for predicting the critical values of coal and gas outbursts using the initial gas flow in a borehole," *Mathematical Problems in Engineering*, vol. 2017, Article ID 7189803, 2017.

[27] S. Peng, J. Xu, H. W. Yang, and D. Liu, "Experimental study on the influence mechanism of gas seepage on coal and gas outburst disaster," *Safety Science*, vol. 50, no. 4, pp. 816–821, 2012.

[28] G. Wang, M. Wu, H. Wang, Q. Huang, and Y. Zhong, "Sensitivity analysis of factors affecting coal and gas outburst based on a energy equilibrium model," *Chinese Journal of Rock Mechanics and Engineering*, vol. 34, no. 2, pp. 1–11, 2015.

[29] J. Xu, D. Liu, S. J. Peng, X. Wu, and Q. Lu, "Experimental research on influence of particle diameter on coal and gas outburst," *Chinese Journal of Rock Mechanics and Engineering*, vol. 29, no. 6, pp. 1231–1237, 2010.

[30] Y. K. Ma, B. S. Nie, X. Q. He, X. C. Li, J. Q. Meng, and D. Z. Song, "Mechanism investigation on coal and gas outburst: an overview," *International Journal of Minerals, Metallurgy and Materials*, vol. 27, no. 7, pp. 872–887, 2020.

[31] K. Wang and Q. X. Yu, "Study on catastrophe theory of the starting process of coal and gas outburst," *China Safety Science Journal*, vol. 8, no. 6, pp. 10–15, 1998.

[32] X. F. Xian, M. Gu, and X. H. Li, "Excitation and occurrence conditions for coal and gas outburst," *Rock and Soil Mechanics*, vol. 30, no. 3, pp. 577–581, 2008.

[33] L. Y. Shu, K. Wang, Q. X. Qi, S. Fan, L. Zhang, and X. Fan, "Key structural body theory of coal and gas outburst," *Chinese Journal of Rock Mechanics and Engineering*, vol. 36, no. 2, pp. 347–356, 2017.

[34] I. Farmer and F. Pooley, "A hypothesis to explain the occurrence of outbursts in coal, based on a study of West Wales outburst coal," *International Journal of Rock Mechanics and Mining Science & Geomechanics Abstracts*, vol. 4, no. 2, pp. 189–193, 1967.

[35] Q. Tu, Y. Cheng, P. Guo, J. Jiang, L. Wang, and R. Zhang, "Experimental study of coal and gas outbursts related to gas-enriched areas," *Rock Mechanics and Rock Engineering*, vol. 49, no. 9, pp. 3769–3781, 2016.

[36] S. N. Zhou and X. Q. He, "Rheological hypothesis of coal and methane outburst mechanism," *Journal of China University of Mining & Technology*, vol. 19, no. 2, pp. 1–8, 1990.

[37] T. Xia, F. Zhou, F. Gao, J. Kang, J. Liu, and J. Wang, "Simulation of coal self-heating processes in underground methane-rich coal seams," *Journal of Coal Geology*, vol. 141, pp. 1–12, 2015.

[38] S. J. Peng, X. W. Song, J. Xu et al., "Experiment of factors affected to coal and gas outburst intensity based on hypothesis of comprehensive effect," *Coal Science and Technology*, vol. 44, no. 12, pp. 81–84, 2016.

[39] C. L. Jiang and Q. X. Yu, "The hypothesis of spherical shell destabilization of coal and gas outburst," *Safety in Coal Mines*, vol. 2, pp. 17–25, 1995.

[40] P. Hou, X. Liang, Y. Zhang, J. He, F. Gao, and J. Liu, "3D multiscale reconstruction of fractured shale and influence of fracture morphology on shale gas flow," *Natural Resources Research*, vol. 30, no. 3, pp. 2463–2481, 2021.

[41] Z. P. Meng, J. Zhang, X. C. Shi, Y. D. Tian, and C. Li, "Calculation model of rock mass permeability in coal mine goaf and its numerical simulation analysis," *Journal of China Coal Society*, vol. 41, no. 8, pp. 1997–2005, 2016.

[42] F. H. An, Y. P. Cheng, L. Wang, and W. Li, "A numerical model for outburst including the effect of adsorbed gas on coal deformation and mechanical properties," *Computers and Geotechnics*, vol. 54, pp. 222–231, 2013.

[43] P. Hou, X. Liang, F. Gao, J. B. Dong, J. He, and Y. Xue, "Quantitative visualization and characteristics of gas flow in 3D pore-fracture system of tight rock based on Lattice Boltzmann simulation," *Journal of Natural Gas Science and Engineering*, vol. 89, no. 4, article 103867, p. 15, 2021.

[44] Y. H. Hu, G. N. Liu, J. Y. Zhu, Y. G. Yang, L. Y. Yu, and F. Gao, "Multiscale and multiphase fractal model considering water reflux in shale gas extraction," *Journal of Natural Gas Science and Engineering*, vol. 101, article 104501, 2022.

[45] D. Kong, Y. Xiong, Z. Cheng, N. Wang, G. Wu, and Y. Liu, "Stability analysis of coal face based on coal face-support-roof system in steeply inclined coal seam," *Geomechanics and Engineering*, vol. 25, no. 3, pp. 233–243, 2021.

[46] M. Gao, S. Zhang, J. Li, and H. Wang, "The dynamic failure mechanism of coal and gas outbursts and response mechanism of support structure," *Thermal Science*, vol. 23, Supplement. 3, pp. 867–875, 2019.

[47] C. Fan, S. Li, D. Elsworth, and Z. Yang, "Experimental investigation on dynamic strength and energy dissipation characteristics of gas outburst-prone coal," *Energy Science and Engineering*, vol. 8, no. 1-4, 2019.

[48] M. J. Liu, X. L. Liu, and J. He, "Research on fractal prediction of coal and gas outburst," *Journal of China Coal Society*, vol. 6, pp. 3–5, 1998.

[49] J. M. Han, Y. Wu, and D. Zhao, "Relationship between methane adsorption and strength about coal sample," *Coal*, vol. 21, no. 1, pp. 12-13, 2012.